The second order perturbation approach for PDEs on random domains

H. Harbrecht, M. Peters

Departement Mathematik und Informatik
Fachbereich Mathematik
Universität Basel
CH-4051 Basel

Preprint No. 2015-40
December 2015

www.math.unibas.ch

THE SECOND ORDER PERTURBATION APPROACH FOR PDES ON RANDOM DOMAINS

H. HARBRECHT AND M. PETERS

Abstract. The present article deals with the solution of boundary value problems on random domains. We apply a second order shape Taylor expansion to approximate the solution's dependence on the random perturbation with third order accuracy in the size of the perturbation's amplitude. The major advantage of this approach is that we end up with deterministic equations for the solution's moments. In particular, representations for the first four moments, i.e., expectation, variance, skewness and kurtosis, are derived. These moments are efficiently computable by means of a boundary element method. Numerical results are presented to illustrate the approach.

1. Introduction

Many problems in science and engineering lead to boundary value problems for an unknown function. Their numerical computation is in general well understood provided that the problem's input parameters are given exactly. Often, however, these input parameters are not known exactly. Hence, one models the uncertain input parameter as a random field which recasts the given boundary value problem into a random one. This in turn yields a solution which is itself a random field.

In this article, we consider the Dirichlet problem for the Poisson equation on a random domain:

$$-\Delta u(\omega) = f \text{ in } D(\omega), \quad u(\omega) = g \text{ on } \partial D(\omega). \tag{1.1}$$

Random domains are motivated by tolerances in the fabrication process of a mechanical device or by damages of the boundary which appear during its life cycle. Such devices are close to a nominal geometry but differ of course from its mathematical

Key words and phrases. Boundary value problem; random domain; perturbation method.

This research has been supported by the Swiss National Science Foundation (SNSF) through the project "$\mathcal{H}$-matrix based first and second moment analysis".

definition. Since tolerances are in general small, we can make the crucial assumption of the smallness of the random perturbations. Uncertainty quantification for computational domains arouses recently more interest, see e.g. [2, 8, 9, 10, 17, 22].

By identifying domains with their boundary, a random domain $D(\omega)$, which is close to the nominal domain D_0, can be seen as a normal perturbation of the nominal boundary ∂D_0:

$$\partial D(\omega) = \{\mathbf{y} \in \mathbb{R}^n : \mathbf{y}(\mathbf{x}) = \mathbf{x} + \varphi(\mathbf{x}, \omega)\mathbf{n}(\mathbf{x}),\ \mathbf{x} \in \partial D_0\}. \tag{1.2}$$

Here, the random field $\varphi(\omega)$ relates to the radius and is a scalar function on ∂D_0. Moreover, $\mathbf{n}$ denotes the outward normal to the domain D_0.

The most simple methodology to deal with randomness is the Monte-Carlo method, see e.g. [14, 20] and the references therein. Numerous draws of the random input data are sampled according to some a-priorily known or empirical distribution. Each draw entails the computation of a deterministic boundary value problem. Then, the statistics like the mean and the variance of these samples is formed. Nevertheless, for boundary values problems on random domains, each sample implies a new domain and thus a new mesh, the assembly of new mass and stiffness matrices, etc. Therefore, the Monte-Carlo method is extremely costly and rather difficult to implement for the problem at hand.

Thus, we aim here at a different approach, namely the perturbation approach, see e.g. [1, 8, 9, 10, 12, 13]. It enables us to approximate the random solution on a fixed domain. The pivotal idea of the perturbation approach for random boundary value problems is the expansion of the underlying random field around the related input parameter's expectation via a (shape-) Taylor series. In case of the random boundary value problem (1.1), this will involve shape calculus, cf. [4, 18, 21]. With the help of the shape Taylor expansion, one can derive asymptotic expansions of the random output's expectation, variance and also higher order moments.

In this article, we employ a second order shape Taylor expansion and derive corresponding asymptotic expansions for the first four moments. These can be computed explicitly under the finite noise assumption. This means, the random domain perturbation in (1.2) is of the form

$$\varphi(\mathbf{x}, \omega) = \sum_{i=1}^{N} \varphi_i(\mathbf{x}) Y_i(\omega) : D_0 \to D(\omega)$$

with centered random variables $Y_i : \Omega \to [-1, 1]$ which are independent and identically distributed. As we will show, the expectation and the variance can be computed

with complexity $\mathcal{O}(N)$. The skewness and kurtosis can be computed with complexity $\mathcal{O}(N^2)$.

The rest of this article is organized as follows. In Section 2, we introduce to shape calculus and derive the asymptotic expansions for the random solution's statistics. Then, in Section 3, we compute these expansions by means of a boundary element method. Numerical results are presented in Section 4. Finally, we state concluding remarks in Section 5

2. Perturbation analysis

To avoid the extreme high-dimensionality of a direct discretization of (1.1), a technique can be applied which is mainly known from shape sensitivity analysis, namely the so-called local shape derivative, cf. [5, 19]. It has been established as a measure of the solution's dependence on domain or boundary perturbations. Such shape derivatives are in principle known since Hadamard, see [7], and nowadays well established in shape optimization, see e.g. [4, 18, 21]. Since the solution's nonlinear dependence on the shape of the domain is Fréchet differentiable, we can linearize around a nominal domain D_0. Thus, deterministic expressions for the solution's statistics can be derived.

2.1. **Shape calculus.** Consider a sufficiently smooth domain D_0 and a boundary variation, for example in the direction of the outward normal $\mathbf{n}$:

$$\mathbf{V} = \varphi\mathbf{n} : \partial D_0 \to \mathbb{R}^n \quad \text{such that} \quad \|\varphi\|_{C^{2,1}(\partial D_0)} \leq 1.$$

Then, the perturbed domain D_ε can be defined as the interior of its boundary

$$\partial D_\varepsilon = \{\mathbf{y} \in \mathbb{R}^n : \mathbf{y}(\mathbf{x}) = \mathbf{x} + \varepsilon\varphi(\mathbf{x})\mathbf{n}(\mathbf{x}),\ \mathbf{x} \in \partial D_0\}.$$

The perturbed domain D_ε is well defined for sufficiently small $\varepsilon > 0$, see also Fig. 2.1 for a visualization.

Using the first and second order local shape derivatives, the solution u_ε of the boundary value problem on the perturbed domain

$$-\Delta u_\varepsilon = f \text{ in } D_\varepsilon, \quad u_\varepsilon = g \text{ on } \partial D_\varepsilon,$$

can be expanded by the shape Taylor expansion

$$u_\varepsilon(\mathbf{x}) = u_0(\mathbf{x}) + \varepsilon\delta u_0[\varphi](\mathbf{x}) + \frac{\varepsilon^2}{2}\delta^2 u_0[\varphi,\varphi](\mathbf{x}) + \mathcal{O}(\varepsilon^3), \quad \mathbf{x} \in K \Subset D_0, \tag{2.3}$$

see [5, 6, 19]. Here, u_0 is the solution of the boundary value problem on the unperturbed domain

$$-\Delta u_0 = f \text{ in } D_0, \quad u_0 = g \text{ on } \partial D_0. \tag{2.4}$$

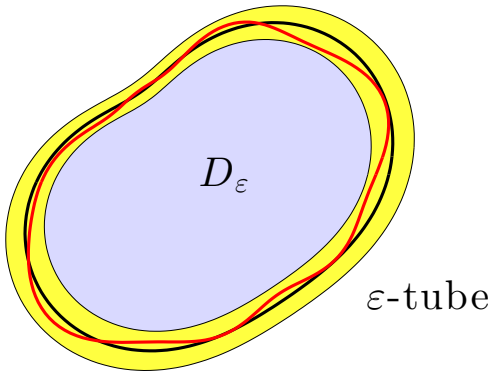

FIGURE 2.1. Illustration of the perturbed domain D_ε.

Moreover, $\delta u_0[\varphi]$ is the first order local shape derivative, which is given by

$$\begin{aligned} \Delta \delta u_0[\varphi] &= 0 && \text{in } D_0, \\ \delta u_0[\varphi] &= \varphi \frac{\partial (g - u_0)}{\partial \mathbf{n}} && \text{on } \partial D_0, \end{aligned} \tag{2.5}$$

and $\delta^2 u_0[\varphi, \varphi']$ is the second order local shape derivative, which is given by

$$\begin{aligned} \Delta \delta^2 u_0[\varphi, \varphi'] &= 0 && \text{in } D_0, \\ \delta^2 u_0[\varphi, \varphi'] &= \varphi \varphi' \frac{\partial^2 (g - u_0)}{\partial \mathbf{n}^2} - \varphi \frac{\partial \delta u_0[\varphi']}{\partial \mathbf{n}} - \varphi' \frac{\partial \delta u_0[\varphi]}{\partial \mathbf{n}} && \text{on } \partial D_0. \end{aligned} \tag{2.6}$$

Notice that the convergence in (2.3) is uniform with respect to $L^\infty(K)$ as $\varepsilon \to 0$ provided that the set K is fixed and contained in D_ε for all sufficiently small $\varepsilon > 0$.

2.2. **Random domains.** We shall now consider random boundary variations. To that end, let $(\Omega, \mathcal{F}, \mathbb{P})$ denote a complete and separable probability space with σ-algebra $\mathcal{F}$ and probability measure $\mathbb{P}$. Here, complete means that $\mathcal{F}$ contains all $\mathbb{P}$-null sets. Then, we define the random perturbation field

$$\mathbf{V}(\omega) = \varphi(\omega)\mathbf{n} : \partial D_0 \to \mathbb{R}^n \quad \text{such that} \quad \|\varphi(\omega)\|_{C^{2,1}(\partial D_0)} \leq 1 \quad \mathbb{P}\text{-almost surely.}$$

For small $\varepsilon > 0$, we thus arrive at the random domain $D_\varepsilon(\omega)$ which is given via its boundary

$$\partial D_\varepsilon(\omega) = \{\mathbf{y} \in \mathbb{R}^n : \mathbf{y}(\mathbf{x}) = \mathbf{x} + \varepsilon \varphi(\mathbf{x}, \omega)\mathbf{n}(\mathbf{x}),\ \mathbf{x} \in \partial D_0\}. \tag{2.7}$$

In view of the first and second order local shape derivatives, the solution $u_\varepsilon(\omega)$ of the random boundary value problem

$$-\Delta u_\varepsilon(\omega) = f \text{ in } D_\varepsilon(\omega), \quad u_\varepsilon(\omega) = g \text{ on } \partial D_\varepsilon(\omega),$$

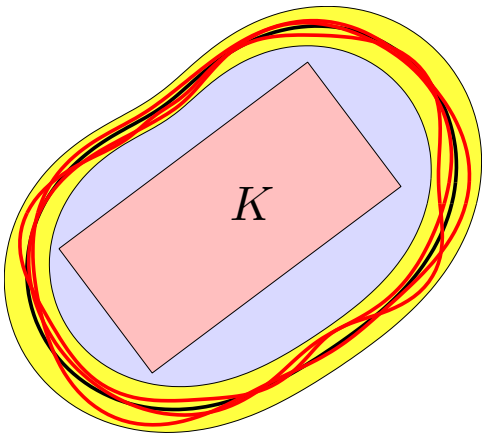

FIGURE 2.2. Illustration of the random domain with evaluation region K.

can be expanded by the shape Taylor expansion

$$u_\varepsilon(\mathbf{x},\omega) = u_0(\mathbf{x}) + \varepsilon\delta u_0(\mathbf{x},\omega) + \frac{\varepsilon^2}{2}\delta^2 u_0(\mathbf{x},\omega) + \mathcal{O}(\varepsilon^3), \quad \mathbf{x} \in K \Subset D_0. \tag{2.8}$$

For notational convenience, we introduce here and in the sequel the abbreviations $\delta u_0(\mathbf{x},\omega) = \delta u_0[\varphi(\omega)](\mathbf{x})$ and $\delta^2 u_0(\mathbf{x},\omega) = \delta^2 u_0[\varphi(\omega),\varphi(\omega)](\mathbf{x})$. In view of the shape Taylor expansion (2.3), we arrive then at the following theorem, see also [10] for the case of first order shape Taylor expansion. A visualization of the random domain with the region K of evaluation is found in Fig. 2.2.

Theorem 2.1. *Assume that the random boundary perturbation φ is centered, i.e. $\mathbb{E}[\varphi](\mathbf{x}) = 0$ for all $\mathbf{x} \in \partial D_0$. Then, for all $\mathbf{x} \in K \Subset D_0$, the expectation and the variance admit the asymptotic expansions*

$$\begin{aligned} \mathbb{E}[u_\varepsilon](\mathbf{x}) &= u_0(\mathbf{x}) + \frac{\varepsilon^2}{2}\mathbb{E}[\delta^2 u_0](\mathbf{x}) + \mathcal{O}(\varepsilon^3), \\ \mathbb{V}[u_\varepsilon](\mathbf{x}) &= \varepsilon^2\mathbb{E}\big[(\delta u_0)^2\big](\mathbf{x}) + \varepsilon^3\mathbb{E}\big[\delta u_0 \delta^2 u_0\big](\mathbf{x}) + \mathcal{O}(\varepsilon^4). \end{aligned} \tag{2.9}$$

Proof. Using the fact that $\mathbb{E}[\delta u_0](\mathbf{x}) = 0$ since $\varphi(\omega)$ is centered, the first equation follows immediately from taking the expectation on both sides of the shape Taylor

expansion (2.8), see [10]. The second equation is obtained in accordance with

$$\begin{aligned}\mathbb{V}[u_\varepsilon] &= \mathbb{E}\big[(u_\varepsilon - \mathbb{E}[u_\varepsilon])^2\big] \\ &= \mathbb{E}\bigg[\bigg(u_0 + \varepsilon\delta u_0 + \frac{\varepsilon^2}{2}\delta^2 u_0 - u_0 - \frac{\varepsilon^2}{2}\mathbb{E}\big[\delta^2 u_0\big] + \mathcal{O}(\varepsilon^3)\bigg)^2\bigg] \\ &= \varepsilon^2\mathbb{E}\bigg[\bigg(\delta u_0 + \frac{\varepsilon}{2}\delta^2 u_0 - \frac{\varepsilon}{2}\mathbb{E}\big[\delta^2 u_0\big]\bigg)^2\bigg] + \mathcal{O}(\varepsilon^4) \\ &= \varepsilon^2\mathbb{E}\big[(\delta u_0)^2\big] + \varepsilon^3\mathbb{E}\big[\delta u_0 \delta^2 u_0\big] + \mathcal{O}(\varepsilon^4),\end{aligned}$$

where we again use that $\mathbb{E}[\delta u_0](\mathbf{x}) = 0$, implying that

$$\mathbb{E}\Big[\delta u_0 \mathbb{E}\big[\delta^2 u_0\big]\Big] = \mathbb{E}[\delta u_0]\mathbb{E}\big[\delta^2 u_0\big] = 0.$$

□

This theorem provides asymptotic expansions of the first two moments which are third and fourth order accurate in the perturbation size ε, respectively. In complete analogy, one can compute asymptotic expansions of the third and fourth moment (and even higher order moments if required).

Corollary 2.2. *The third centered moment is given by*

$$\begin{aligned}\mathbb{M}_3[u_\varepsilon](\mathbf{x}) &= \mathbb{E}\Big[\big(u_\varepsilon(\mathbf{x}) - \mathbb{E}[u_0](\mathbf{x})\big)^3\Big] = \varepsilon^3\mathbb{E}\Big[\big(\delta u_0(\mathbf{x})\big)^3\Big] \\ &\quad + \frac{3\varepsilon^4}{2}\mathbb{E}\Big[\big(\delta u_0(\mathbf{x})\big)^2\Big(\delta^2 u_0(\mathbf{x}) - \mathbb{E}\big[\delta^2 u_0(\mathbf{x})\big]\Big)\Big] + \mathcal{O}(\varepsilon^5)\end{aligned} \tag{2.10}$$

and the fourth centered moment is given by

$$\begin{aligned}\mathbb{M}_4[u_\varepsilon](\mathbf{x}) &= \mathbb{E}\Big[\big(u_\varepsilon(\mathbf{x}) - \mathbb{E}[u_0](\mathbf{x})\big)^4\Big] = \varepsilon^4\mathbb{E}\Big[\big(\delta u_0(\mathbf{x})\big)^4\Big] \\ &\quad + 2\varepsilon^5\mathbb{E}\Big[\big(\delta u_0(\mathbf{x})\big)^3\Big(\delta^2 u_0(\mathbf{x}) - \mathbb{E}\big[\delta^2 u_0(\mathbf{x})\big]\Big)\Big] + \mathcal{O}(\varepsilon^6).\end{aligned} \tag{2.11}$$

2.3. **Computation of the asymptotic expansions.** Let us assume that the random field be given in form of the expansion

$$\varphi(\mathbf{x},\omega) = \sum_{i=1}^{N} \varphi_i(\mathbf{x}) Y_i(\omega), \tag{2.12}$$

where the random variables $Y_i : \Omega \to [-1,1]$ are centered, independent and identically distributed and where the spatial coefficient functions $\{\varphi_i\}_i$ form a subset of $C^{2,1}(\overline{D_0})$. Notice that, if $\varphi(\mathbf{x},\omega)$ is not centered, we can redefine the reference domain D_0 as the interior of the boundary

$$\partial\widetilde{D}_0 = \{\mathbf{y} \in \mathbb{R}^n : \mathbf{y}(\mathbf{x}) = \mathbf{x} + \mathbb{E}[\varphi](\mathbf{x})\mathbf{n}(\mathbf{x}),\ \mathbf{x} \in \partial D_0\}.$$

The random perturbations are then centered with respect to the transformed reference domain $\widetilde{D}_0$.

Lemma 2.3. *Let $\varphi(\mathbf{x},\omega)$ be given by (2.12). Then, there holds*

$$\delta u_0[\varphi(\mathbf{x},\omega)] = \sum_{i=1}^{N} \delta u_0[\varphi_i](\mathbf{x}) Y_i(\omega)$$

and

$$\delta^2 u_0[\varphi(\mathbf{x},\omega),\varphi(\mathbf{x},\omega)] = \sum_{i,j=1}^{N} \delta^2 u_0[\varphi_i,\varphi_j](\mathbf{x}) Y_i(\omega) Y_j(\omega).$$

Proof. The claim for the first order local shape derivative follows directly the linearity of the first order local shape derivative with the representation (2.12). For the second order local shape derivative, the assertion is obtained from its bilinearity, again, together with the representation (2.12) for the random field. □

With this lemma at hand, together with the multinomial theorem where $\boldsymbol{\alpha} = (\alpha_1,\dots,\alpha_N)$ denotes an N-dimensional multiindex, we derive

$$\begin{aligned}
\mathbb{E}\big[(\delta u_0)^k\big](\mathbf{x}) &= \mathbb{E}\bigg[\bigg(\sum_{i=1}^{N} \delta u_0[\varphi_i](\mathbf{x}) Y_i\bigg)^k\bigg] \\
&= \mathbb{E}\bigg[\sum_{|\boldsymbol{\alpha}|=k} \binom{k}{\boldsymbol{\alpha}} \prod_{i=1}^{N} \big(\delta u_0[\varphi_i](\mathbf{x}) Y_i\big)^{\alpha_i}\bigg] \\
&= \sum_{|\boldsymbol{\alpha}|=k} \binom{k}{\boldsymbol{\alpha}} \prod_{i=1}^{N} \big(\delta u_0[\varphi_i](\mathbf{x})\big)^{\alpha_i} \mathbb{E}\bigg[\prod_{i=1}^{N} Y_i^{\alpha_i}\bigg].
\end{aligned}$$

In order to obtain expressions for the first order local shape derivative's moments up to order four, we discuss these cases now explicitly. As we will see, the expressions become more involved for increasing k due to the increasing number of possible configurations for $|\boldsymbol{\alpha}| = k$.

- For $k = 1$, we have only the situation $\{\alpha_i = 1\}$ for one $i \in \{1,\dots,N\}$ and thus, due to the centeredness of the Y_i, that
$$\mathbb{E}\bigg[\prod_{i=1}^{N} Y_i^{\alpha_i}\bigg] = 0.$$
- In the case $k = 2$, we face the situations $\{\alpha_i = 1, \alpha_j = 1\}$ and $\{\alpha_i = 2\}$ for distinct $i,j \in \{1,\dots,N\}$. This results in
$$\mathbb{E}\bigg[\prod_{i=1}^{N} Y_i^{\alpha_i}\bigg] = \mathbb{V}[Y_i] \quad \text{if } \alpha_i = 2$$

Otherwise, we end up with $\mathbb{E}\big[\prod_{i=1}^N Y_i^{\alpha_i}\big] = 0$ by the independence of the random variables.

- For $k = 3$, we have the situations $\{\alpha_i = 1, \alpha_j = 1, \alpha_k = 1\}$, $\{\alpha_i = 2, \alpha_j = 1\}$ and $\{\alpha_i = 3\}$ for distinct $i, j, k \in \{1, \dots, N\}$. Again, the independence and the centeredness imply that $\mathbb{E}\big[\prod_{i=1}^N Y_i^{\alpha_i}\big] = 0$ in the first two cases. In the third case, we obtain

$$\mathbb{E}\bigg[\prod_{i=1}^N Y_i^{\alpha_i}\bigg] = \mathbb{E}[Y_i^3] \quad \text{if } \alpha_i = 3.$$

- Finally, for $k = 4$, we face the situations $\{\alpha_i = 1, \alpha_j = 1, \alpha_k = 1, \alpha_\ell = 1\}$, $\{\alpha_i = 2, \alpha_j = 1, \alpha_k = 1\}$, $\{\alpha_i = 2, \alpha_j = 2\}$, $\{\alpha_i = 3, \alpha_j = 1\}$ and $\{\alpha_i = 4\}$ for distinct $i, j, k, \ell \in \{1, \dots, N\}$. In cases one and three, the independence and the centeredness of the random variables imply that $\mathbb{E}\big[\prod_{i=1}^N Y_i^{\alpha_i}\big] = 0$. Thus, we finally obtain

$$\mathbb{E}\bigg[\prod_{i=1}^N Y_i^{\alpha_i}\bigg] = \begin{cases} \mathbb{V}[Y_i]\mathbb{V}[Y_j] & \text{if } \alpha_i = \alpha_j = 2, \\ \mathbb{E}[Y_i^4] & \text{if } \alpha_i = 4. \end{cases}$$

By combining these computations, we conclude

Lemma 2.4. *For random fields of the form* (2.12)*, it holds*

$$\mathbb{E}\big[(\delta u_0)^k\big](\mathbf{x}) = \begin{cases} 0, & k = 1, \\ \mathbb{V}[Y] \sum_{i=1}^N \big(\delta u_0[\varphi_i](\mathbf{x})\big)^2, & k = 2, \\ \mathbb{E}\big[Y^3\big] \sum_{i=1}^N \big(\delta u_0[\varphi_i](\mathbf{x})\big)^3, & k = 3, \\ \big(\mathbb{E}\big[Y^4\big] - 3\mathbb{V}[Y]^2\big) \sum_{i=1}^N \big(\delta u_0[\varphi_i](\mathbf{x})\big)^4 + 3\big(\mathbb{E}\big[(\delta u_0)^2\big](\mathbf{x})\big)^2, & k = 4. \end{cases}$$

Notice that the aforementioned equations are also feasible to compute the terms

$$\mathbb{E}\big[(\delta u_0)^k \mathbb{E}[\delta^2 u_0]\big](\mathbf{x}) = \mathbb{E}\big[(\delta u_0)^k\big](\mathbf{x}) \cdot \mathbb{E}[\delta^2 u_0](\mathbf{x})$$

for $k = 2, 3$ which appear in the asymptotic expansions (2.10) and (2.11) of the third and fourth centered moments.

Another term we shall provide is $\mathbb{E}\big[(\delta u_0)^k \delta^2 u_0\big](\mathbf{x})$ for $k = 0, 1, 2, 3$. It can be computed in complete analogy by employing Lemma 2.3. We find

$$\begin{aligned}
&\mathbb{E}\big[(\delta u_0)^k \delta^2 u_0\big](\mathbf{x}) \\
&\quad = \mathbb{E}\bigg[\sum_{|\boldsymbol{\alpha}|=k} \binom{k}{\boldsymbol{\alpha}} \prod_{\ell=1}^{N} \big(\delta u_0[\varphi_\ell](\mathbf{x}) Y_\ell\big)^{\alpha_\ell} \sum_{i,j=1}^{N} \delta^2 u_0[\varphi_i, \varphi_j](\mathbf{x}) Y_i Y_j \bigg] \\
&\quad = \sum_{|\boldsymbol{\alpha}|=k} \binom{k}{\boldsymbol{\alpha}} \prod_{\ell=1}^{N} \big(\delta u_0[\varphi_\ell](\mathbf{x})\big)^{\alpha_\ell} \sum_{i,j=1}^{N} \delta^2 u_0[\varphi_i, \varphi_j](\mathbf{x}) \mathbb{E}\bigg[Y_i Y_j \prod_{\ell=1}^{N} Y_\ell^{\alpha_\ell} \bigg].
\end{aligned}$$

In view of the previous computations and

$$|\boldsymbol{\alpha}| = 5 \quad \Longrightarrow \quad \mathbb{E}\bigg[\prod_{i=1}^{N} Y_i^{\alpha_i} \bigg] = \begin{cases} \mathbb{V}[Y_i]\mathbb{E}[Y_j^3], & \text{if } \alpha_i = 2,\ \alpha_j = 3, \\ \mathbb{E}[Y_i^3]\mathbb{V}[Y_j], & \text{if } \alpha_i = 3,\ \alpha_j = 2, \\ \mathbb{E}[Y_i^5], & \text{if } \alpha_i = 5, \\ 0, & \text{otherwise,} \end{cases}$$

straightforward calculation yields

Lemma 2.5. *For random fields of the form* (2.12)*, it holds*

$$\begin{aligned}
&\mathbb{E}\big[(\delta u_0)^k \delta^2 u_0\big](\mathbf{x}) \\
&\quad = \begin{cases}
\mathbb{V}[Y] \sum_{i=1}^{N} \delta^2 u_0[\varphi_i, \varphi_i](\mathbf{x}), & \text{if } k = 0, \\
\mathbb{E}\big[Y^3\big] \sum_{i=1}^{N} \delta u_0[\varphi_i](\mathbf{x}) \delta^2 u_0[\varphi_i, \varphi_i](\mathbf{x}), & \text{if } k = 1, \\
\Big(\mathbb{E}\big[Y^4\big] - 3\big(\mathbb{V}[Y]\big)^2\Big) \sum_{i=1}^{N} \big(\delta u_0[\varphi_i](\mathbf{x})\big)^2 \delta^2 u_0[\varphi_i, \varphi_i](\mathbf{x}) \\
\quad + \mathbb{E}\big[(\delta u_0)^2\big](\mathbf{x}) \mathbb{E}\big[\delta^2 u_0\big](\mathbf{x}) \\
\quad + 2\big(\mathbb{V}[Y]\big)^2 \sum_{i,j=1}^{N} \delta u_0[\varphi_i](\mathbf{x}) \delta u_0[\varphi_j](\mathbf{x}) \delta^2 u_0[\varphi_i, \varphi_j](\mathbf{x}), & \text{if } k = 2, \\
\Big(\mathbb{E}\big[Y^5\big] - 10\mathbb{V}\big[Y^2\big]\mathbb{E}\big[Y^3\big]\Big) \sum_{i=1}^{N} \big(\delta u_0[\varphi_i](\mathbf{x})\big)^2 \delta^2 u_0[\varphi_i, \varphi_i](\mathbf{x}) \\
\quad + \mathbb{E}\big[(\delta u_0)^3\big](\mathbf{x}) \mathbb{E}\big[\delta^2 u_0\big](\mathbf{x}) \\
\quad + 3\,\mathbb{E}\big[(\delta u_0)^2\big](\mathbf{x}) \mathbb{E}\big[\delta u_0 \delta^2 u_0\big](\mathbf{x}) \\
\quad + 6\,\mathbb{E}\big[Y^3\big]\mathbb{V}[Y] \sum_{i,j=1}^{N} \big(\delta^2 u_0[\varphi_i](\mathbf{x})\big)^2 \delta u_0[\varphi_j](\mathbf{x}) \delta^2 u_0[\varphi_i, \varphi_j](\mathbf{x}), & \text{if } k = 3.
\end{cases}
\end{aligned}$$

To summarize, we have provided by now easily computable expressions that are feasible to evaluate the asymptotic expansions for the expectation and the variance in accordance with (2.9), as well as the skewness (2.10) and the kurtosis (2.11). The computational complexity is $\mathcal{O}(N)$ for the expectation and the variance while the computational complexity is $\mathcal{O}(N^2)$ for the third and fourth centered moment.

Remark 2.6. *If the law of Y is symmetric, then it holds $\mathbb{E}\big[Y(\omega)^3\big] = 0$ and $\mathbb{E}\big[Y(\omega)^5\big] = 0$. Consequently, the asymptotic expansion of the variance simplifies in accordance with*

$$\mathbb{V}[u_\varepsilon](\mathbf{x}) = \varepsilon^2\mathbb{E}\Big[\big(\delta u_0(\mathbf{x},\omega)\big)^2\Big](\mathbf{x}) + \mathcal{O}(\varepsilon^4), \quad \mathbf{x} \in K \Subset D_0.$$

The equations for the third and fourth centered moment become simpler correspondingly, see (4.24) *for the particular case of the uniform distribution.*

3. Boundary integral equations

We shall explain now how we compute the solution u_0 to the boundary value problem (2.4) and the associated local shape derivatives $\delta u_0[\varphi]$ and $\delta^2 u_0[\varphi]$ given by (2.5) and (2.6), respectively. In order to compute first and second order normal derivates of the solution u_0 to (2.4), we will employ the boundary element method. For sake of simplicity in representation, we restrict ourselves from now on to the two-dimensional situation, i.e., $n = 2$. Nevertheless, we emphasize that the three-dimensional situation can be treated in complete analogy.

3.1. **Newton potential.**

In order to apply the boundary element method to the Poisson equation with non-homogenous loading, we make the ansatz

$$u_0 = v + N_f \tag{3.13}$$

for a suitable Newton potential N_f which satisfies the equation $-\Delta N_f = f$ and a harmonic function v which satisfies the boundary value problem

$$\Delta v = 0 \text{ in } D_0, \quad v = g - N_f \text{ on } \partial D_0. \tag{3.14}$$

The Newton potential has to be given analytically or computed in advance in a possibly fairly simple domain $\widehat{D}$ which contains the domain D_0 under consideration. Hence, efficient solution techniques for the Poisson equation, like e.g. a multigrid method, can easily be applied, see [11].

3.2. **Dirichlet-to-Neumann map.** Our approach to determine the solution v of the Laplace equation (3.14) relies on the reformulation as a boundary integral equation by using Green's function for the underlying differential operator. Namely, the solution $v(\mathbf{x})$ of (3.14) is given in each point $\mathbf{x} \in D_0$ by the representation formula

$$v(\mathbf{x}) = \int_{\partial D_0} \left\{ G(\mathbf{x},\mathbf{y}) \frac{\partial v}{\partial \mathbf{n}}(\mathbf{y}) - \frac{\partial G(\mathbf{x},\mathbf{y})}{\partial \mathbf{n}_\mathbf{y}} v(\mathbf{y}) \right\} \mathrm{d}\sigma_\mathbf{y}. \tag{3.15}$$

Taking into account the jump properties of the layer potentials, we obtain the direct boundary integral formulation of the problem

$$\frac{1}{2} v(\mathbf{x}) = \int_{\partial D_0} G(\mathbf{x},\mathbf{y}) \frac{\partial v}{\partial \mathbf{n}}(\mathbf{y}) \, \mathrm{d}\sigma_\mathbf{y} - \int_{\partial D_0} \frac{\partial G(\mathbf{x},\mathbf{y})}{\partial \mathbf{n}_\mathbf{y}} v(\mathbf{y}) \, \mathrm{d}\sigma_\mathbf{y},$$

where $\mathbf{x} \in \partial D_0$. Introducing the single layer operator

$$\mathcal{V} : H^{-1/2}(\partial D_0) \to H^{1/2}(\partial D_0), \quad \big(\mathcal{V}\rho\big)(\mathbf{x}) = -\frac{1}{2\pi} \int_{\partial D_0} \log \|\mathbf{x}-\mathbf{y}\| \, \rho(\mathbf{y}) \, \mathrm{d}\sigma_\mathbf{y} \tag{3.16}$$

and the double layer operator

$$\mathcal{K} : L^2(\partial D_0) \to L^2(\partial D_0), \quad \big(\mathcal{K}\rho\big)(\mathbf{x}) = \frac{1}{2\pi} \int_{\partial D_0} \frac{\langle \mathbf{x}-\mathbf{y}, \mathbf{n}_\mathbf{y} \rangle}{\|\mathbf{x}-\mathbf{y}\|^2} \rho(\mathbf{y}) \, \mathrm{d}\sigma_\mathbf{y} \tag{3.17}$$

and incorporating the Dirichlet boundary condition $u = g - N_f$ on ∂D, we arrive at the boundary integral equation

$$\mathcal{V} \frac{\partial v}{\partial \mathbf{n}} = \left(\frac{1}{2\pi} + \mathcal{K} \right) (g - N_f) \quad \text{on } \partial D_0. \tag{3.18}$$

This is the Neumann-to-Dirichlet map for the harmonic function v. The boundary integral operator on the left hand side is symmetric and $H^{-1/2}(\partial D_0)$-elliptic provided that $\operatorname{diam}(\partial D_0) < 1$. This is sufficient to ensure the unique solvability of the integral equation.

3.3. **Computing the first order local shape derivate.** The Neumann data of the local shape derivative $\delta u_0[\varphi]$ are easily computable by applying again the Dirichlet to Neumann map:

$$\mathcal{V} \frac{\partial \delta u_0[\varphi]}{\partial \mathbf{n}} = \left(\frac{1}{2\pi} + \mathcal{K} \right) \left(\varphi \frac{\partial (g - v - N_f)}{\partial \mathbf{n}} \right) \quad \text{on } \partial D_0. \tag{3.19}$$

Then, in complete analogy to (3.15), the local shape derivative at the point $\mathbf{x} \in D_0$ is given by

$$\delta u_0[\varphi](\mathbf{x}) = \int_{\partial D_0} \left\{ G(\mathbf{x},\mathbf{y}) \frac{\partial \delta u_0[\varphi]}{\partial \mathbf{n}}(\mathbf{y}) - \frac{\partial G(\mathbf{x},\mathbf{y})}{\partial \mathbf{n}_\mathbf{y}} \left(\varphi(\mathbf{y}) \frac{\partial (g - v - N_f)}{\partial \mathbf{n}}(\mathbf{y}) \right) \right\} \mathrm{d}\sigma_\mathbf{y}.$$

3.4. **Computing the second order local shape derivate.** The Dirichlet boundary data of the second order local shape derivate involve the term $\partial^2 u_0/\partial \mathbf{n}^2$. Its computation is explained in the following lemma.

Lemma 3.1. *There hold the identity*

$$\frac{\partial^2 u_0}{\partial \mathbf{n}^2} = -\frac{\partial^2 g}{\partial \mathbf{t}^2} - \kappa \left(\frac{\partial v}{\partial \mathbf{n}} - \frac{\partial (g - N_f)}{\partial \mathbf{n}} \right) - f,$$

where κ denotes the curvature of ∂D_0.

Proof. Due to $u_0 = v + N_f$, we have to prove that

$$\frac{\partial^2 v}{\partial \mathbf{n}^2} = -\frac{\partial^2 (g - N_f)}{\partial \mathbf{t}^2} - \kappa \left(\frac{\partial v}{\partial \mathbf{n}} - \frac{\partial (g - N_f)}{\partial \mathbf{n}} \right).$$

To this end, let $\boldsymbol{\gamma} : [0, 2\pi] \to \partial D_0$ denote a regular parametric representation of the boundary ∂D_0. Then, we obtain the formulas

$$\mathbf{t}(s) = \frac{\boldsymbol{\gamma}'(s)}{\|\boldsymbol{\gamma}'(s)\|}, \quad \kappa(s) = -\frac{\langle \boldsymbol{\gamma}''(s), \mathbf{n}(s) \rangle}{\|\boldsymbol{\gamma}'(s)\|^2},$$

and $\partial/\partial \mathbf{t} = \partial/(\|\boldsymbol{\gamma}'\| \partial s)$. From

$$\begin{aligned} \frac{\partial^2 v}{\partial s^2} &= \frac{\partial}{\partial s} \langle \nabla v, \boldsymbol{\gamma}' \rangle \\ &= \langle \nabla^2 v \cdot \boldsymbol{\gamma}', \boldsymbol{\gamma}' \rangle + \langle \nabla v, \boldsymbol{\gamma}'' \rangle \\ &= \|\boldsymbol{\gamma}'\|^2 \frac{\partial^2 v}{\partial \mathbf{t}^2} + \langle \boldsymbol{\gamma}'', \mathbf{t} \rangle \frac{\partial v}{\partial \mathbf{t}} + \langle \boldsymbol{\gamma}'', \mathbf{n} \rangle \frac{\partial v}{\partial \mathbf{n}} \end{aligned}$$

we conclude on the one hand that

$$\frac{\partial^2 v}{\partial \mathbf{t}^2} = \frac{1}{\|\boldsymbol{\gamma}'\|^2} \frac{\partial^2 v}{\partial s^2} - \frac{\langle \boldsymbol{\gamma}'', \mathbf{t} \rangle}{\|\boldsymbol{\gamma}'\|^2} \frac{\partial v}{\partial \mathbf{t}} - \frac{\langle \boldsymbol{\gamma}'', \mathbf{n} \rangle}{\|\boldsymbol{\gamma}'\|^2} \frac{\partial v}{\partial \mathbf{n}}. \tag{3.20}$$

On the other hand, we can compute $\partial^2 v/\partial s^2$ from the boundary condition $g - N_f$:

$$\frac{\partial^2 v}{\partial s^2} = \|\boldsymbol{\gamma}'\|^2 \frac{\partial^2 (g - N_f)}{\partial \mathbf{t}^2} + \langle \boldsymbol{\gamma}'', \mathbf{t} \rangle \frac{\partial (g - N_f)}{\partial \mathbf{t}} + \langle \boldsymbol{\gamma}'', \mathbf{n} \rangle \frac{\partial (g - N_f)}{\partial \mathbf{n}}.$$

The assertion follows now by inserting this relation into (3.20) and observing that

$$\frac{\partial^2 v}{\partial \mathbf{t}^2} + \frac{\partial^2 v}{\partial \mathbf{n}^2} = \Delta v = 0,$$

which holds true since $v \in C^2(\overline{D_0})$. □

Since the second order local shape derivative has only to be known inside the domain D_0, we can use the indirect ansatz

$$\delta^2 u_0[\varphi, \varphi'](\mathbf{x}) = \int_{\partial D_0} G(\mathbf{x}, \mathbf{y}) \rho(\mathbf{y}) \, \mathrm{d}\sigma_{\mathbf{y}}, \quad \mathbf{x} \in D_0.$$

The unknown density $\rho \in H^{-1/2}(\partial D_0)$ is given by the first kind integral equation

$$\mathcal{V}\rho = \varphi\varphi' \frac{\partial^2 (g-u_0)}{\partial \mathbf{n}^2} - \varphi \frac{\partial \delta u_0[\varphi']}{\partial \mathbf{n}} - \varphi' \frac{\partial \delta u_0[\varphi]}{\partial \mathbf{n}} \quad \text{on } \partial D_0. \tag{3.21}$$

3.5. **Solving boundary integral equations.** The next step towards the solution of the boundary value problem is the numerical approximation of the integral operators included in (3.18), (3.19) and (3.21), which first requires the parametrization of the integral operators. To that end, we insert a parametrization $\boldsymbol{\gamma} : [0, 2\pi] \to \partial D_0$ of the boundary ∂D_0. For the approximation of the unknown Cauchy data, we use the collocation method based on trigonometric polynomials. Applying the trapezoidal rule for the numerical quadrature and the regularization technique along the lines of [15] to deal with the singular integrals, we arrive at an exponentially convergent boundary element method provided that the data and the boundaries and thus the solution are arbitrarily smooth.

4. Numerical results

For the numerical examples, we consider the Poisson equation

$$-\Delta u(\omega) = 1 \text{ in } D_\varepsilon(\omega), \quad u(\omega) = 0 \text{ on } \partial D_\varepsilon(\omega), \tag{4.22}$$

on the randomly varying disc

$$D_\varepsilon(\omega) = \Big\{ \big(\rho(\phi)\cos(\phi), \rho(\phi)\sin(\phi)\big) \in \mathbb{R}^2 : \\ 0 \le \rho(\phi) < r(\phi,\omega) = \frac{2}{5} + \frac{\varepsilon}{80} \sum_{\ell=1}^{5} Y_{2\ell}(\omega)\cos(\ell\phi) + Y_{2\ell-1}(\omega)\sin(\ell\phi) \Big\}$$

with $\varepsilon \le 1/2$ and independent random variables $Y_1, \dots, Y_{10} \sim \mathcal{U}([-1,1])$. The nominal domain D_0 is thus the disc of radius $2/5$:

$$D_0 = \Big\{ \big(\rho(\phi)\cos(\phi), \rho(\phi)\sin(\phi)\big) \in \mathbb{R}^2 : 0 \le \rho(\phi) < \frac{2}{5},\ 0 \le \phi < 2\pi \}.$$

A visualization of different realizations of the randomly varying domain in case of $\varepsilon = 1/2$ is found in Figure 4.3.

One readily verifies that the moments of the random variables satisfy

$$\mathbb{E}[Y_\ell^k] = \begin{cases} 0, & \text{if } k \text{ odd}, \\ \frac{1}{k+1}, & \text{if } k \text{ even}. \end{cases}$$

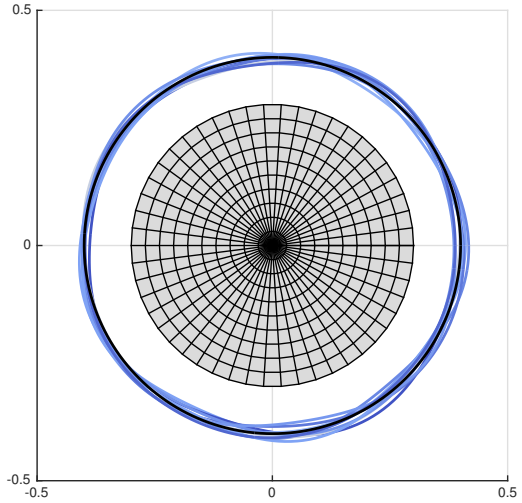

FIGURE 4.3. Different realizations of the domain $D_{1/2}(\omega)$ with inscribed non-varying compactum K.

Consequently, we obtain along the lines of Lemmata 2.4 and 2.5 the expansions

$$\begin{aligned}\mathbb{E}[u_\varepsilon](\mathbf{x}) &= u_0(\mathbf{x}) + \frac{\varepsilon^2}{6}\sum_{i=1}^N \delta^2 u_0[\varphi_i,\varphi_i](\mathbf{x}) + \mathcal{O}(\varepsilon^3),\\ \mathbb{V}[u_\varepsilon](\mathbf{x}) &= \frac{\varepsilon^2}{6}\sum_{i=1}^N \big(\delta u_0[\varphi_i](\mathbf{x})\big)^2 + \mathcal{O}(\varepsilon^4),\end{aligned} \tag{4.23}$$

for the expectation and variance. Whereas, for the skewness and the kurtosis, we arrive at

$$\begin{aligned}\mathbb{M}_3[u_\varepsilon](\mathbf{x}) = \frac{3\varepsilon^4}{2}\Bigg[&\frac{2}{9}\sum_{i,j=1}^N \delta u_0[\varphi_i](\mathbf{x})\delta u_0[\varphi_j](\mathbf{x})\delta^2 u_0[\varphi_i,\varphi_j](\mathbf{x})\\ &- \frac{2}{15}\sum_{i=1}^N \big(\delta u_0[\varphi_i](\mathbf{x})\big)^2\delta^2 u_0[\varphi_i,\varphi_i](\mathbf{x})\Bigg] + \mathcal{O}(\varepsilon^5),\\ \mathbb{M}_4[u_\varepsilon](\mathbf{x}) = \varepsilon^4\Bigg[\frac{1}{3}\Bigg(\sum_{i=1}^N \big(\delta u_0[\varphi_i](\mathbf{x})\big)^2\Bigg)^2 &- \frac{2}{15}\sum_{i=1}^N \big(\delta u_0[\varphi_i](\mathbf{x})\big)^4\Bigg] + \mathcal{O}(\varepsilon^6).\end{aligned} \tag{4.24}$$

For varying ε, we will compare these asymptotic expansions with results derived by a quasi-Monte Carlo approximation based on the Halton sequence with 10^5 samples. To that end, we evaluate the samples on the compactum $K = \{\mathbf{x} \in \mathbb{R}^2 : \|\mathbf{x}\|_2 \leq 0.3\}$ in order to compute the solution's first four moments. Notice that, for all $\varepsilon \leq 0.5$, the compactum K is almost surely contained in $D_\varepsilon(\omega)$, see also Figure 4.3.

The computation of the solution u_0 of the unperturbed problem and the associated first and second order local shape derivaties are computed as introduced in Section 3 by employing 200 collocation points. The numerical solution of (4.22) for the particular samples is likewise determined by using the Dirichlet-to-Neumann map. A suitable Newton potential for (4.22) is given by the function

$$N_f(\mathbf{x}) = -\frac{1}{4}(x_1^2 + x_2^2).$$

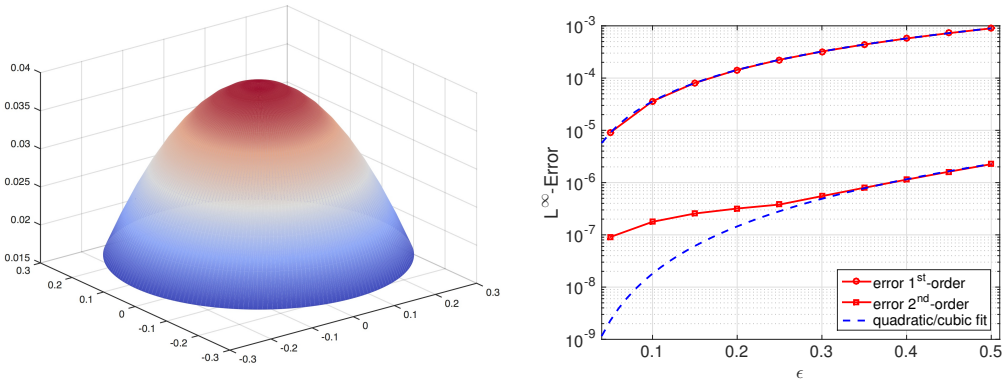

FIGURE 4.4. Visualization of the mean in case of $\varepsilon = 1/2$ and the asymptotic behavior of the asymptotic expansion.

Figure 4.4 shows a visualization of the approximate mean in case of $\varepsilon = 1/2$ on the left hand side. On the right hand side, the asymptotic behaviour of the perturbation approach is presented in terms of the approximate mean's L^∞-error. It is evaluated on a grid similar to that one depicted in Figure 4.3 with about 2000 points. As a comparison, we also depicted the results which would be obtained by a first order shape Taylor expansion, resulting in the approximation $\mathbb{E}[u_\varepsilon](\mathbf{x}) = u_0(\mathbf{x}) + \mathcal{O}(\varepsilon^2)$. As it turns out, the first order perturbation approach perfectly provides the predicted quadratic rate, indicated by the dashed line. Here and in the sequel, the polynomial fits are obtained by a least squares fit of the coefficient of the respective monomial. For the second order perturbation approach, the cubic rate is not entirely visible. This may be caused by a lack of precision in the quasi-Monte Carlo reference. Nevertheless, we observe an error that is two to three orders of magnitude smaller then the error for the first order approach.

As can be derived from (4.23), the first and second order perturbation approach coincide in case of the variance since the third order term just vanishes due to the symmetry of the random variables' distribution. A visualization of the approximate variance in case of $\varepsilon = 1/2$ can be found on the left hand side of Figure 4.7. Whereas,

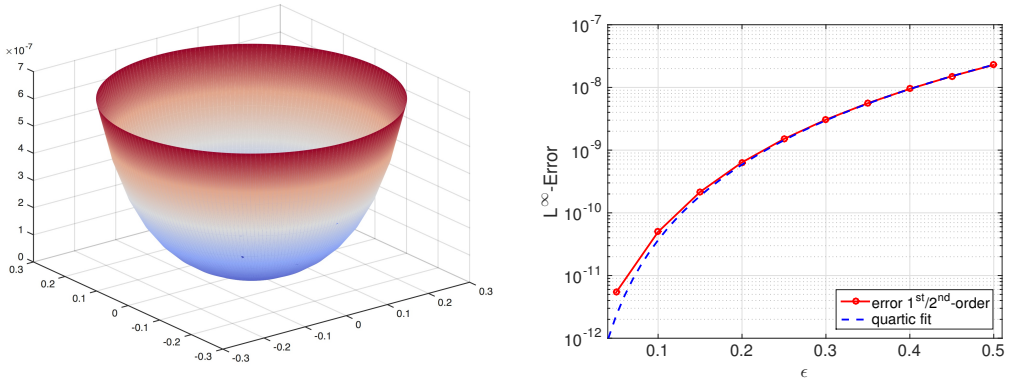

FIGURE 4.5. Visualization of the variance in case of $\varepsilon = 1/2$ and the asymptotic behavior of the asymptotic expansion.

the asymptotic rate for the L^∞-error of the approximate variation is shown on the right hand side of Figure 4.7. As can be seen, the error perfectly reflects the quartic fit.

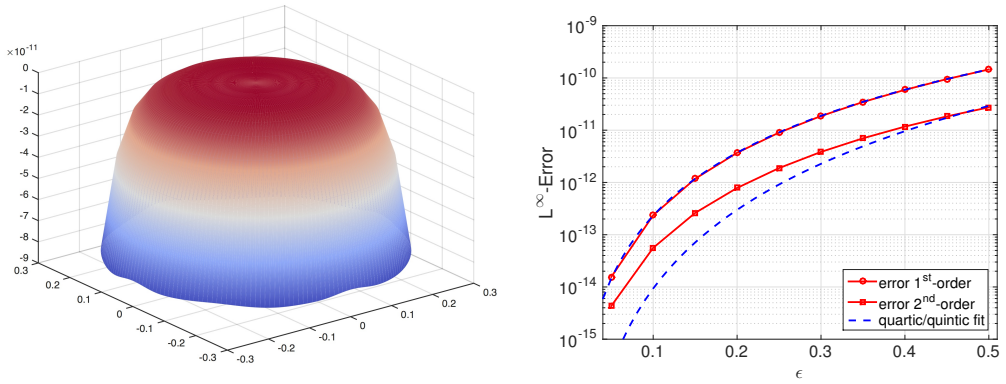

FIGURE 4.6. Visualization of the skewness in case of $\varepsilon = 1/2$ and the asymptotic behavior of the asymptotic expansion.

The next moment to be considered is the random solution's skewness. On the left hand side of Figure 4.6, we find a visualization of the skewness in case of $\varepsilon = 1/2$. The right hand side of Figure 4.6 contains the corresponding error for different sizes of ε. In difference to (2.10), the first order perturbation approach amounts to the expansion $\mathbb{M}_3[u_\varepsilon](\mathbf{x}) = \mathcal{O}(\varepsilon^4)$. Indeed, we exactly observe this quartic rate in our computations. Compared to this, the expansion of the second order perturbation approach is up to one order of magnitude more precise. Nevertheless, the expected quintic rate is not entirely met.

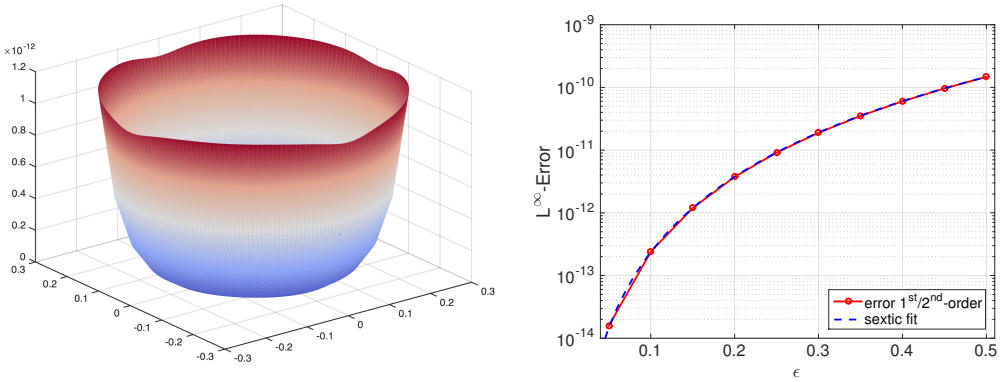

FIGURE 4.7. Visualization of the kutorsis in case of $\varepsilon = 1/2$ and the asymptotic behavior of the asymptotic expansion.

Finally, we consider the random solution's kurtosis. It is depicted on the left hand side of Figure 4.7 for the choice $\varepsilon = 1/2$. As in the case of the variance, the first and second order perturbation approach coincide due to the symmetry of the random variables. As can be seen in the right hand side of Figure 4.7, the asymptotic expansion's error exhibits the predicted sextic rate.

5. Conclusion

In the present article, we have applied the second order perturbation approach to boundary value problems that are defined with respect to random domains. To that end, we have derived asymptotic expansions for the expectation, the variance, the skewness and the kurtosis. In particular, we developed a boundary element method to efficiently compute these expansions. By numerical experiments, we have demonstrated that the second order perturbation approach is much more accurate than the first order perturbation approach, particularly when computing the expectation.

References

[1] I. Babuška and P. Chatzipantelidis. On solving elliptic stochastic partial differential equations. *Comput. Meth. Appl. Mech. Engrg.* **191** (2002) 4093–4122.

[2] C. Canuto and T. Kozubek. A fictitious domain approach to the numerical solution of PDEs in stochastic domains. *Numer. Math.* **107** (2007) 257–293.

[3] J.E. Castrillon-Candas, F. Nobile, R.F. Tempone. Analytic regularity and collocation approximation for PDEs with random domain deformations. *MATHICSE Technical report 45.2013*, EPF Lausanne, Switzerland, 2013.

[4] M. Delfour and J.-P. Zolesio. *Shapes and Geometries*. SIAM, Philadelphia, 2001.

[5] K. Eppler. Optimal shape design for elliptic equations via BIE-methods. *Int. J. Appl. Math. Comput. Sci.* **10** (2000) 487–516.

[6] K. Eppler. Boundary integral representations of second derivatives in shape optimization. *Discuss. Math. Differ. Incl. Control Optim.* **20** (2000) 63–78.

[7] J. Hadamard. *Lectures on the Calculus of Variations*. Gauthier–Villiars, Paris, 1910.

[8] H. Harbrecht. On output functionals of boundary value problems on stochastic domains. *Math. Meth. Appl. Sci.* **33** (2010) 91–102.

[9] H. Harbrecht and J. Li. First order second moment analysis for stochastic interface problems based on low-rank approximation. *ESAIM Math. Model. Numer. Anal.* **47** (2013) 1533–1552.

[10] H. Harbrecht, R. Schneider, and C. Schwab. Sparse second moment analysis for elliptic problems in stochastic domains. *Numer. Math.* **109** (2008) 167–188.

[11] M. Jung and O. Steinbach. A finite element-boundary element algorithm for inhomogeneous boundary value problems. *Computing* **68** (2002) 1–17.

[12] J.B. Keller. *Stochastic Equations and Wave Propagation in Random Media*. Bellman, 1964.

[13] M. Kleiber and T.D. Hien. *The Stochastic Finite Element Method: Basic Perturbation Technique and Computer Implementation*. Wiley, 1992.

[14] P.E. Kloeden and E. Platen. *Numerical Solution of Stochastic Differential Equations*. Springer-Verlag, 3rd ed., 1999.

[15] R. Kress. *Linear Integral Equations*. Vol. 82 of Applied Mathematical Sciences, Springer, New York, 2nd ed., 1999.

[16] M. Loève. *Probability Theory. I+II*. Volume 45 of Graduate Texts in Mathematics. Springer, Berlin-Heidelberg-New York, 4th ed., 1977.

[17] P.S. Mohan, P.B. Nair, and A.J. Keane. Stochastic projection schemes for deterministic linear elliptic partial differential equations on random domains. *Int. J. Numer. Meth. Engng.* **85** (2011) 874–895.

[18] O. Pironneau. *Optimal Shape Design for Elliptic Systems*. Springer, New York, 1984.

[19] R. Potthast. Frechét–Differenzierbarkeit von Randintegraloperatoren und Randwertproblemen zur Helmholtzgleichung und zu den zeitharmonischen Maxwellgleichungen. *PhD thesis*, Georg–August–Universität Göttingen, 1994.

[20] P. Protter. *Stochastic Integration and Differential Equations: A New Approach*. 3rd edition, Springer, 1995.

[21] J. Sokolowski and J.-P. Zolesio. *Introduction to Shape Optimization: Shape Sensitivity Analysis*. Springer, 1992.

[22] D.M. Tartakovsky and D. Xiu. Numerical methods for differential equations in random domains. *SIAM J. Sci. Comput.* **28** (2006) 1167–1185.

Helmut Harbrecht, Michael Peters, Universität Basel, Departement Mathematik und Informatik, Spiegelgasse 1, 4051 Basel, Schweiz

E-mail address: {helmut.harbrecht,michael.peters}@unibas.ch

LATEST PREPRINTS

No.	Author: *Title*
2015-21	**A. Schikorra** *Nonlinear Comutators for the fractional p-Laplacian and applications*
2015-22	**L. Martinazzi** *Fractional Adams-Moser-Trudinger type inequalities*
2015-23	**P. Habegger, J. Pila** *O-Minimality and certain atypical intersections*
2015-24	**P. Habegger** *Singular Moduli that are Algebraic Units*
2015-25	**P. Habegger, F. Pazuki** *Bad Reduction of genus 2 curves with CM jacobian varieties*
2015-26	**A. Bohun, F. Bouchut, G. Crippa** *Lagrangian solutions to the 2D Euler system with L^1 vorticity and infinite energy*
2015-27	**A.-L. Haji-Ali, H. Harbrecht, M. Peters, M. Siebenmorgen** *Novel results for the anisotropic sparse quadrature and their impact on random diffusion problems*
2015-28	**P. Habegger, G. Jones, D. Masser** *Six unlikely intersection problems in search of effectivity*
2015-29	**M. Griebel, H. Harbrecht, M. Peters** *Multilevel quadrature for elliptic parametric partial differential equations on non-nested meshes*
2015-30	**M. J. Grote, M. Kray, F. Nataf, F. Assous** *Time-dependent wave splitting and source separation*
2015-31	**T. Boulenger, D. Himmelsbach, E. Lenzmann** *Blowup for fractional NLS*
2015-32	**A. Hyder** *Moser functions and fractional Moser-Trudinger type inequalities*
2015-33	**S. Zimmermann** *The Cremona group of the plane is compactly presented*

Preprints are available under *https://math.unibas.ch/research/publications*

LATEST PREPRINTS

No.	Author: *Title*
2015-34	**S. Zimmermann** *The Abelianisation of the real Cremona group*
2015-35	**J. Dölz, H. Harbrecht, M. Peters** *H-matrix based second moment analysis for rough random fields and finite element discretizations*
2015-36	**J. K. Canci** *Good reduction for endomorphisms of the projective line in terms of the branch locus*
2015-37	**J. K. Canci, L. Paladino** *Preperiodic points for rational functions defined over a global field in terms of good reduction*
2015-38	**J. K. Canci** *Preperiodic points for rational functions defined over a rational function field of characteristic zero*
2015-39	**J. K. Canci, S. Vishkautsan** *Quadratic maps with a periodic critical point of period 2*
2015-40	**H. Harbrecht, M. Peters** *The second order perturbation approach for PDEs on random domains*
